



Some reflections on reflectors and wave amplitudes

Nathalie Favretto-Cristini, Paul Cristini, Eric de Bazelaire

► To cite this version:

Nathalie Favretto-Cristini, Paul Cristini, Eric de Bazelaire. Some reflections on reflectors and wave amplitudes. *Acta Acustica united with Acustica*, 2007, 93 (6), pp.909-916. hal-00462465

HAL Id: hal-00462465

<https://hal.science/hal-00462465>

Submitted on 29 Jan 2014

HAL is a multi-disciplinary open access archive for the deposit and dissemination of scientific research documents, whether they are published or not. The documents may come from teaching and research institutions in France or abroad, or from public or private research centers.

L'archive ouverte pluridisciplinaire **HAL**, est destinée au dépôt et à la diffusion de documents scientifiques de niveau recherche, publiés ou non, émanant des établissements d'enseignement et de recherche français ou étrangers, des laboratoires publics ou privés.

Some Reflections on Reflectors and Wave Amplitudes

Nathalie Favretto-Cristini, Paul Cristini

Laboratoire de Modélisation et Imagerie en Géosciences (MIGP), CNRS, Université de Pau et des Pays de l'Adour, BP 1155, 64013 Pau, France. nathalie.favretto@univ-pau.fr

E. De Bazelaire*

11, Route du bourg, 64230 Beyrie-en-Béarn, France

Summary

The paper describes the reflector from a seismic viewpoint, and investigates the imprint of such a description on the wave reflection process. More specifically, the spatial region in the vicinity of the interface which actually affects the reflected wavefield is determined using the Fresnel volume and the Interface Fresnel zone (IFZ) concepts. This region is represented by a volume of integration of properties above and below the interface whose maximum lateral extent corresponds to the lateral extent of the IFZ, and whose maximum vertical extent corresponds to a thickness we evaluate accurately and which can be greater than the seismic wavelengths. Considering this description of a reflector, we then calculate the amplitude of the P-wave emanating from a point source and recorded at a receiver after its specular reflection on a smooth homogeneous interface between two elastic media. As the problem under consideration can be viewed as a problem of diffraction by the IFZ which is the physically relevant part of the interface which actually affects the reflected wavefield in this simple case, we then apply the Angular Spectrum Approach (ASA) combined with the IFZ concept to get the 3D analytical solution. The variation in the reflected P-wave amplitude evaluated with the ASA, as a function of the incidence angle, is finally compared with the plane-wave reflection coefficient, and with the exact solution obtained with the 3D code OASES. Below but close to the critical angle, the prediction of our approximation better fits the exact solution than the plane-wave reflection coefficient, which emphasizes the importance of accounting for the IFZ in amplitude calculations even for a very simple elastic model.

PACS no. 43.20.Gp, 91.30.Ab

Introduction

In seismic reflection surveys the waves generated by a point source propagate in the stratified Earth, and are recorded at the surface by the receivers, after being reflected by the reflectors (or, more generally speaking, interfaces). Analysis of the seismic data provides information on the medium characteristics. Provided the velocity model of the medium is known, analysis of the travel-times provides the reflector location, while from the waveforms we can get information on the physical properties of the medium. Nevertheless, retrieving the geometrical and physical characteristics of the Earth is actually a difficult task, since the medium can be highly complex and heterogeneous, depending on the seismic frequency range of interest. Since many decades geophysicists have therefore developed various theoretical methods to fit the real seismic data. Most of them are based on approximations

of wave propagation processes and on assumptions on the geological model. One of the approximations consists in neglecting the effect of the laterally varying properties of the interfaces. However, recorded data bear the marks of the heterogeneities located in the medium body, and also the marks of the heterogeneities located at the interfaces. Our ultimate goal is therefore to evaluate the imprint of the interface properties on the recorded seismic data. Except for mathematical convenience, interfaces are not infinitely thin. The underlying questions are then: What is a reflector like from the seismic and physical viewpoints? In other words, considering an isolated interface, how thick are the regions above and beyond the interface which actually affect the reflected wavefield recorded by the receivers? What is the imprint of these regions on the interface reflectivity and on the amplitudes of the reflected waves? In the paper we focus on these questions.

The basis of many seismic studies is the ray theory [1]. Under this approximation it is assumed that the high-frequency part of elastic energy propagates along infinitely narrow lines through space, called rays, which join the source and the receiver. Ray theory is then strictly valid

Received 25 January 2007, revised 20 July 2007,
accepted 20 August 2007.

* Deceased on 28 June 2007

only in the limit of a hypothetical infinite-frequency wave. As recorded seismic data have a low frequency content (typically, between 10 and 60 Hz), it is accepted that seismic wave propagation is extended to a finite volume of space around the ray path, called the 1st Fresnel volume [2], which contributes to the received wavefield for each frequency. The first Fresnel volume, hereafter denoted FV, and its intersection with a reflector, called the Interface Fresnel zone (IFZ), have received broad attention in recent past years. These concepts are continually being developed and have found so many applications in seismology and in seismic exploration, that it is impossible here to review all the books and articles which pay attention to them in seismic wave propagation [3, 4, 5]. Nevertheless, we shall mention the works of Červený and his co-authors who have suggested two methods for including FV parameter calculations into the ray tracing procedure in complex 2D and 3D structures. The first one, called the Fresnel volume ray tracing [6], combines the paraxial ray approximation with the dynamic ray tracing, and is only applicable to zero-order waves (direct, reflected and transmitted waves...), whereas the second method, more accurate than the previous one, is based on network ray tracing [7]. They have also derived analytical expressions for FVs of seismic body waves and for IFZ for simple structures, which offers a deeper insight into the properties of FV and IFZ [8, 9]. Of particular interest are the size of the IFZ and the size of the volume of the reflector involved in reflection time measurements [10], because each one can be related to the horizontal and vertical resolutions of seismic methods [11, 12]. Unfortunately, as Červený and co-authors' objectives were concerned essentially with kinematic ray tracing, the expressions they derived are incomplete. Until now, only the IFZ and the penetration depth of the FV below the reflector were considered in studies. Nevertheless, if the seismic amplitudes at receivers have to be evaluated, we must determine the interface reflectivity by accounting for the spatial region in the vicinity of the interface which affects it. In other words, we must account for the IFZ and for certain volumes below the interface in the transmission medium and above the interface in the incidence medium. The goal of the paper is to define the reflector from the seismic viewpoint, and thus to obtain a better understanding of the process of wave reflection from the reflector.

The paper is organized in two sections. Section 1 is concerned with the seismic description of a reflector. Special attention is paid to the FV and to the IFZ which are frequency-dependent, and which also depend on the position of the source and the receivers. We then determine the part of the reflector which actually affects the reflected wavefield. Section 2 investigates the role of the IFZ in the reflected wave propagation. To focus specifically on the imprint of the IFZ, we consider a very simple elastic model, e.g. a smooth homogeneous interface between homogeneous, isotropic, and elastic media. Heterogeneities at the interface will be the scope of future works. We introduce the method we used for deriving the amplitude of the P-wave, emanating from a point source and recorded at the

receiver after its reflection on the interface. As the problem under consideration can be viewed as a problem of diffraction by the IFZ, i.e. in this case the physically relevant part of the interface which actually affects the reflected wavefield, we applied the Angular Spectrum Approach (ASA) [13] to get the 3D analytical solution. Finally, the variation in the reflected P-wave amplitude, as a function of the incidence angle, evaluated with the ASA is compared with the classical plane-wave (PW) reflection coefficient, and with the exact solution obtained with the 3D code OASES (<http://acoustics.mit.edu/faculty/henrik/oases.html>).

1. Seismic amplitude: contribution of the interface and of its near volume

We assume that the interface is isolated from the other ones. We mean that the distance between this interface and another one is much greater than $\frac{V}{2B}$, where V is the medium velocity and B is the frequency bandwidth of the source. Consequently, there is no interference between close interfaces.

1.1. Maximum lateral extension of the contributing volume

We consider two homogeneous isotropic elastic media in welded contact at a plane interface located at a distance z_M from the xy -plane including the point source $S(x_S, 0, 0)$, and the receiver $R(x_R, 0, 0)$. The source generates in the upper medium a spherical wave with a constant amplitude. The spherical wave can be decomposed into an infinite sum of plane waves (PW), synchronous each other at the time origin. We consider the harmonic PW with frequency f which propagates in the upper medium with the velocity V_{P1} from S to R , after being reflected by the interface at the point $M(0, 0, z_M)$ in a specular direction θ with respect to the normal to the interface (Figure 1). Let the traveltime of the specular reflected wave be t_{SMR} .

The set of all possible rays SM_iR with constant traveltime t_{SMR} defines the isochrone for the source-receiver pair (S, R) relative to the specular reflection SMR . This isochrone describes an ellipsoid of revolution tangent to the interface at M , whose rotational axis passes through S and R . By definition, the FV corresponding to S and R , and associated with the reflection at M , is formed by virtual diffraction points F such that the waves passing through these points interfere constructively with the specular reflected wave. This condition is fulfilled when the path-length difference is less than one-half of the wavelength $\lambda_1 = \frac{V_{P1}}{f}$ corresponding to the dominant frequency f of the narrow-band source signal [2]:

$$|l(F, S) + l(F, R) - l(M, S) - l(M, R)| \leq \frac{\lambda_1}{2}, \quad (1)$$

the quantity $l(X, Y)$ denoting the distance between the point X and the point Y . As is well-known, the main contribution to the wavefield comes from the first FV as the rapid oscillatory responses of the higher-order FVs and Fresnel

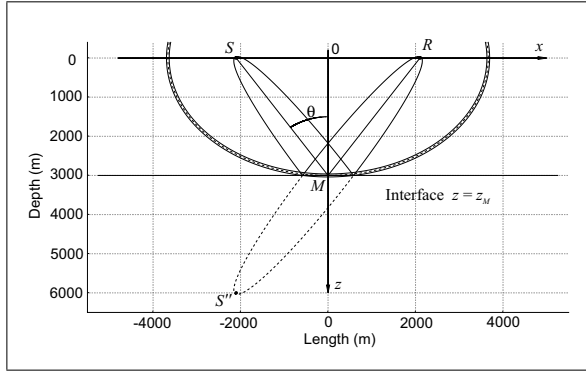


Figure 1. Representations, in the xz -plane, of the Fresnel volume involved in the wave reflection at the point M at a plane interface, under the incidence angle $\theta = 35^\circ$. The source S and the receiver R are situated at a distance 3000 m from the interface. The classical representation of the Fresnel volume is the ellipsoid of revolution with foci located at R and at the image source S' . This representation, mainly based on transmission considerations, is suitable for accounting for the heterogeneities located in the medium body. Another representation of the Fresnel volume associated with the reflection SMR is given by the volume located in the incidence medium between the ellipsoids of revolution with foci at S and R (see the text for more details). This representation is appropriate for accounting for the heterogeneities in the vicinity of the interface. The velocities in the upper and lower media are respectively $V_{P1} = 4000$ m/s and $V_{P2} = 5200$ m/s, and the frequency $f = 32$ Hz. The seismic wavelengths in the upper and lower media are respectively $\lambda_1 = 125$ m and $\lambda_2 = 162.5$ m. The critical angle is equal to $\theta_C = 50.28^\circ$.

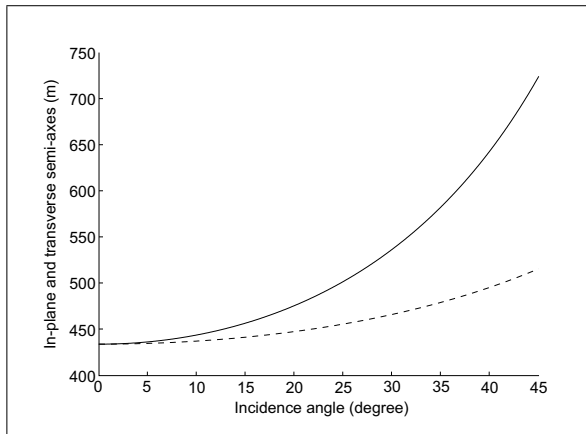


Figure 2. Variation in the in-plane semi-axis r^{\parallel} (—) and in the transverse semi-axis r^{\perp} (---) of the Interface Fresnel zone as a function of the incidence angle θ . The velocities in the upper and lower media are respectively $V_{P1} = 4000$ m/s and $V_{P2} = 5200$ m/s, and the frequency $f = 32$ Hz. The seismic wavelengths in the upper and lower media are respectively $\lambda_1 = 125$ m and $\lambda_2 = 162.5$ m. The critical angle is equal to $\theta_C = 50.28^\circ$.

zones cancel out and give minor contributions to the wavefield [14]. In our work we restrict ourselves to the first FV which is simply referred to as FV. The FV is represented by the volume situated above the interface in the upper medium and bounded by two ellipsoids of revolution, with

foci at S and R , tangent to fictitious parallel planes to the interface and located at a distance $\frac{\lambda_1}{4}$ below and above the interface (Figure 1). The two ellipsoids of revolution are defined by:

$$\frac{x^2}{(z_M / \cos \theta \pm \lambda_1 / 4)^2} + \frac{y^2}{(z_M / \cos \theta \pm \lambda_1 / 4)^2 - z_M^2 \tan^2 \theta} + \frac{z^2}{(z_M / \cos \theta \pm \lambda_1 / 4)^2 - z_M^2 \tan^2 \theta} - 1 = 0. \quad (2)$$

Here, it must be specified that, as seismic wavefields are transient and large-band, it is generally necessary to decompose the source signal into narrow-band signals for which monochromatic FV can be constructed for the prevailing frequency of the signal spectrum [15].

The IFZ is defined as the cross section of the FV by an interface which may not be perpendicular to the ray SM . If the source S and the receiver R are situated at the same distance from the interface, the IFZ is represented by an ellipse centered at the reflection point M , whose equation is obtained from the formulation of the ellipsoid of revolution, equation (2), keeping the sign $+$ and replacing z by z_M . The in-plane semi-axis r^{\parallel} and the transverse semi-axis r^{\perp} of the IFZ are then expressed as:

$$r^{\parallel} = \sqrt{\left[\frac{\lambda_1}{2} \left(\frac{z_M}{\cos \theta} + \frac{\lambda_1}{8} \right) \right] \cdot \left[1 - \frac{z_M^2 \tan^2 \theta}{\left(\frac{z_M}{\cos \theta} + \frac{\lambda_1}{4} \right)^2} \right]^{-1}},$$

$$r^{\perp} = \sqrt{\frac{\lambda_1}{2} \left(\frac{z_M}{\cos \theta} + \frac{\lambda_1}{8} \right)}. \quad (3)$$

The characteristics of the IFZ depend on the positions of the source-receiver pair, and also on the incidence angle of the ray SM . Moreover, larger portions of the interface are involved for low-frequency than for high-frequency components of the wavefield, and also for great incidence angles θ rather than for small angles (Figure 2). It is also well-known that a perturbation of the medium actually affects the reflected wave when this perturbation is located inside the IFZ.

Expressions for the semi-axes of the IFZ associated with the reflected wavefield, given by equation (3), are identical to those reported in [8]. Here, we must clarify some important points. In many papers is used the classical representation of the FV which is an ellipsoid of revolution with foci located at R and at the mirror image S' of the source S (Figure 1). This representation, mainly based on transmission considerations, is suitable for accounting for the heterogeneities of the medium body located in the vicinity of the ray, while the FV representation we use is more appropriate to account for the heterogeneities of the interface, as it is connected strictly to the wave reflection process. Moreover, unlike the classical one, this representation allows the definition of the volumes above and beyond the interface which characterize the reflector. The following subsection is focused on this definition. Note that the two representations are complementary and must be combined

if the wave propagation in media with heterogeneities in the body and at the interfaces is investigated.

1.2. Maximum vertical extension of the contributing volume

It is well-known that the FV of the reflected wave is not limited by the interface, but penetrates across the interface in the transmission medium. The penetration distance can be evaluated approximately in an analytical way following travelttime measurements or in a numerical way using the network ray tracing [8]. We propose to define it accurately in the plane of symmetry between S and R for subcritical incidence angles.

The transmission law of curvature described in [16, p.43]:

$$K_2 = K_1 \frac{V_{P2}}{V_{P1}} \left(\frac{\cos \theta}{\cos \theta'} \right)^2 + \frac{K}{\cos \theta'} \left(\frac{V_{P2}}{V_{P1}} \frac{\cos \theta}{\cos \theta'} - 1 \right), \quad (4)$$

connects the curvature K_2 of the transmitted wavefront to the curvature K_1 of the incident wavefront and to the interface curvature K . The transmission angle θ' is connected to the incidence angle θ through Snell's law, and V_{P2} denotes the velocity in the lower medium. In the case of a plane interface ($K = 0$), the transmission law of curvature, equation (4), becomes in terms of radii of curvature R_2 and R_1 :

$$R_2 = R_1 \frac{V_{P1}}{V_{P2}} \left(\frac{\cos \theta'}{\cos \theta} \right)^2. \quad (5)$$

By substituting the radii of curvature R_2 and R_1 for their respective expression $\frac{z_M}{\cos \theta}$ and $\frac{z_{S'}}{\cos \theta'}$, we get the position of the new fictitious source-receiver pair (S', R') with respect to the interface plane $z = z_M$, as a function of the incidence angle θ :

$$z_{R'} = z_{S'} = z_M \frac{V_{P1}}{V_{P2}} \left(\frac{\cos \theta'}{\cos \theta} \right)^3. \quad (6)$$

The pair (S', R') which can be viewed as image of (S, R) for the transmission process would provide the same wavefront curvature as (S, R), but occurring entirely in the transmission medium. As previously, by considering the ellipsoid of revolution with foci S' and R' , tangent to the interface plane at M, and the new ellipsoids which define the FV associated with the reflection $S'MR'$ (Figure 3), it is straightforward to evaluate the penetration distance D_2 of the FV of the reflected wave, in the transmission medium, in the plane of symmetry between S and R:

$$D_2 = \left(z_{S'}^2 + \frac{\lambda_2 z_{S'}}{2 \cos \theta'} + \frac{\lambda_2^2}{16} \right)^{\frac{1}{2}} - z_{S'}. \quad (7)$$

This result is valid only for subcritical incidence angles θ and in the plane of symmetry between S and R. For $\theta = 0$, the distance D_2 equals the well-known value $\frac{\lambda_2}{4}$

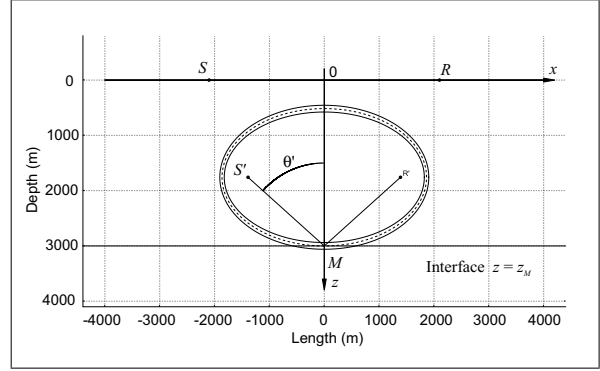


Figure 3. Representation, in the xz -plane, of the Fresnel volume involved in the fictitious wave reflection at the point M of the plane interface, under the incidence angle θ' . The fictitious source-receiver pair (S', R'), located at a distance $z_{S'}$ from the interface plane, can be viewed as image of the pair (S, R) and would provide the same wavefront curvature as (S, R), but occurring entirely in the transmission medium. The velocities in the upper and lower media are respectively $V_{P1} = 4000$ m/s and $V_{P2} = 5200$ m/s, and the frequency $f = 32$ Hz. The seismic wavelengths in the upper and lower media are respectively $\lambda_1 = 125$ m and $\lambda_2 = 162.5$ m.

[8]. The penetration distance D_2 increases with increasing incidence angles, but is always smaller than the seismic wavelength λ_2 (Figure 4). The penetration distance, out of the plane of symmetry, can be also evaluated in the same way from the envelope of the ellipsoids of revolution with foci S' and R' moving along caustics, even for non-planar interfaces ($K \neq 0$). Nevertheless, for postcritical incidence angles, as total reflection occurs, we are not able to define the penetration distance of the FV below the interface by using the transmission law of curvature. Note that the approximation of the distance D_2 given in [8] can be obtained for values of the incidence angle θ close to zero, and then for great position $z_{S'}$, by deriving a 1st-order approximation of the expression (7) of D_2 with respect to $(1/z_{S'}^2)(\lambda_2 z_{S'}/2 \cos \theta' + \lambda_2/8)$. This approximation overestimates the real value of the distance D_2 , and its accuracy decreases with increasing incidence angles (Figure 4).

Following the same reasoning, it is clear that a region above the interface in the incidence medium also contributes actually to the reflected wavefield. This region has got thickness D_1 in the plane of symmetry between S and R which can be evaluated in the same way as previously, the pair (S'', R'') being viewed as image of (S, R) with respect to the interface plane:

$$D_1 = \left(z_M^2 + \frac{\lambda_1 z_M}{2 \cos \theta} + \frac{\lambda_1^2}{16} \right)^{\frac{1}{2}} - z_M. \quad (8)$$

This result is exact in the plane of symmetry between S and R whatever the incidence angle θ . For $\theta = 0$, the distance D_1 equals the value $\frac{\lambda_1}{4}$. The thickness D_1 increases with increasing incidence angles and is always smaller than the seismic wavelength λ_1 and the penetration distance D_2

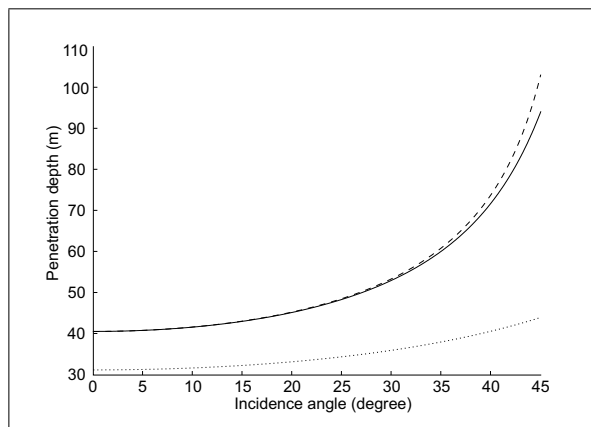


Figure 4. Variation in the penetration depth D_1 of the Fresnel volume above the interface (.....) and in the penetration depth D_2 below the interface (—) as a function of the incidence angle θ . Comparison with the variation in the penetration depth D_2 (- - -) provided by Kvasnička and Červený's approximation as a function of the incidence angle θ . The velocities in the upper and lower media are respectively $V_{P1} = 4000$ m/s and $V_{P2} = 5200$ m/s, and the frequency $f = 32$ Hz. The seismic wavelengths in the upper and lower media are respectively $\lambda_1 = 125$ m and $\lambda_2 = 162.5$ m. The critical angle is equal to $\theta_C = 50.28^\circ$.

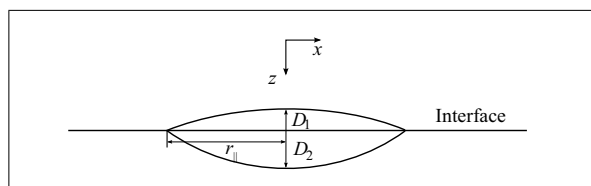


Figure 5. Seismic description of a reflector in the xz -plane. The in-plane semi-axis of the Interface Fresnel zone is denoted by r_{\parallel} . The distance D_1 is the maximum thickness of the region above the interface which affects the reflected wavefield, whereas the distance D_2 characterizes the penetration distance of the Fresnel volume (associated with the reflected wave) below the interface in the transmission medium, in the plane of symmetry between the source and the receiver.

(Figure 4). The distance D_1 , out of the plane of symmetry, can be also evaluated exactly in the same way because the caustics along which the foci S'' and R'' move are degenerate and are then reduced to points.

We are now able to define what a reflector is like from the seismic and physical viewpoints. A reflector is a volume of integration of properties above and below the interface. This volume is represented by the regions with maximum thicknesses D_1 and D_2 in the plane of symmetry between the source and the receiver (Figure 5). Its maximum lateral extent corresponds to the lateral extent of the IFZ, and its maximum vertical extent corresponds to the thickness $D = D_1 + D_2$ which can be greater than the seismic wavelengths.

Here, we must clarify some points. If amplitude measurements are considered, the interface reflectivity has to be determined by considering this volume which actually

affects it. For the evaluation of the interface reflectivity, the structural description of the multi-scaled heterogeneities located in the regions above and below the interface has to be considered as a preliminary step toward the forward modeling of the response of the interface. Our future contributions will be focused on this topic. On the other hand, if only traveltime measurements are considered, for instance, for locating the reflectors in the media, there is no need for defining the region above the interface with thickness D_1 , because this region is already included in the classical representation of the FV. In this case, only the region beyond the interface with thickness D_2 has to be considered.

2. Application

The aim of this section is to investigate the imprint of the reflector described previously on the wave reflection process. More specifically, we want to evaluate its influence on the calculation of the amplitude of the reflected wave measured at the receiver. For this purpose, it is instructive to compare the variation in the amplitude obtained with a method which accounts for the physical description of the reflector, as a function of the incidence angle, with the amplitude predicted by a numerical code which provides the exact solution, and with the amplitude predicted by the classical PW theory (here, the Zoeppritz equations [17]). To focus specifically on the imprint of accounting for the FV concept, we consider a very simple elastic model, e.g. a smooth homogeneous interface between homogeneous, isotropic, and elastic media. As there is no heterogeneity in the vicinity of the interface, and more specially in the regions above and below the interface which describe the reflector, only the IFZ has to be considered for the computation of the amplitude of the reflected wave.

2.1. Medium, model and exact solution

Let the orthotropic source be located at the point S, far from the plane interface between the media. The spherical P-wave emanating from the source propagates obliquely in the upper medium and strikes the homogeneous interface. It is then reflected from the interface and finally measured at the receiver located at the point R, far from the interface.

One case of interface between elastic media whose properties are reported in Table I has been chosen to illustrate the theoretical results. The interface is situated at a distance $z_M = 3000$ m from the source-receiver plane. The source spectrum is chosen to be the Fourier transform of a Ricker wavelet with the dominant frequency $f = 32$ Hz and the frequency bandwidth $\Delta f = 8$ Hz.

We used the 3D code OASES¹ to compute accurately synthetic seismograms in media. OASES is a general purpose computer code for modeling seismo-acoustic propagation in horizontally stratified media using wavenumber integration in combination with the Direct Global Matrix solution technique [18, 19, 20]. This software has

¹ <http://acoustics.mit.edu/faculty/henrik.oases.html>

Table I. Properties of the homogeneous, isotropic and elastic media in contact. ρ , V_P and V_S denote, respectively, the density, P-wave and S-wave velocities for the upper (subscript 1 in the text) and lower (subscript 2 in the text) media.

Properties	V_P (m/s)	V_S (m/s)	ρ (kg/m ³)
Upper medium	4000	2000	2000
Lower medium	5200	2500	2400

the great advantage of providing reference solutions for various types of sources (explosive source, vertical point force, etc...). In addition, upward and downward propagation of compressional and of shear waves can be easily separated. This 3D code is widely used in the underwater acoustics community and has been thoroughly validated.

2.2. Angular Spectrum Approach combined with IFZ

The problem under consideration can be viewed as a problem of diffraction by the physically relevant part of the interface (namely, the IFZ). We chose to apply the Angular Spectrum Approach (ASA) [13] combined with the IFZ concept to get the 3D analytical solution to this problem. The motivations of this choice are twofold. Provided the incident spherical wavefield is decomposed by Fourier analysis into a linear combination of elementary plane wavesurfaces, traveling in different directions away from the source, the effect of propagation over distance is simply a change of the relative phases of the various plane wavesurface components. Sherman [21] has proved that despite their apparent differences, the ASA and the first Rayleigh-Sommerfeld solution [13, chapter 3 page 47] yield identical predictions of diffracted fields. The advantage of using the ASA then seems obvious: it permits straightforward derivations of the measured amplitude of the reflected wave at the point R. We refer to the book of Goodman [13, chapter 3 pages 55-61] for a detailed treatment of the ASA.

When using the ASA, we have to remind that it is a technique for modeling the propagation of acoustic fields between parallel planes. Therefore, considering the case of the reflection of fields from an oblique interface requires the following successive stages:

- stage 1: calculation of the spherical P-wavefield emanating from the point source S which has propagated in the upper medium, only inside the IFZ at the interface. Nullification of the wavefield outside the IFZ,
- stage 2: 2D Fast Fourier Transformation of the wavefield in order to obtain its angular spectrum,
- stage 3: application of the PW reflection coefficient (here, the P-P reflection coefficient),
- stage 4: rotational transformation of complex amplitudes in the Fourier domain and interpolation [22],
- stage 5: propagation of the angular spectrum,
- stage 6: 2D inverse Fast Fourier Transformation of the angular spectrum, in order to get the amplitude of the reflected P-wave measured at the receiver.

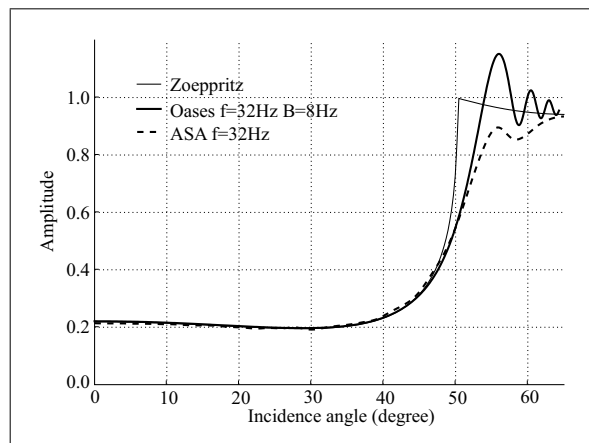


Figure 6. Variation in the amplitude of the P-wave reflected from a plane interface, as a function of the incidence angle. Comparison between the plane-wave reflection coefficient and the spreading-free amplitudes associated with the exact solution and with the approximate solution. The exact solution is provided by the 3D code OASES, whereas the approximate solution is obtained by applying the Angular Spectrum Approach together with the Interface Fresnel Zone concept. (See Table I and text for the description of the medium configuration).

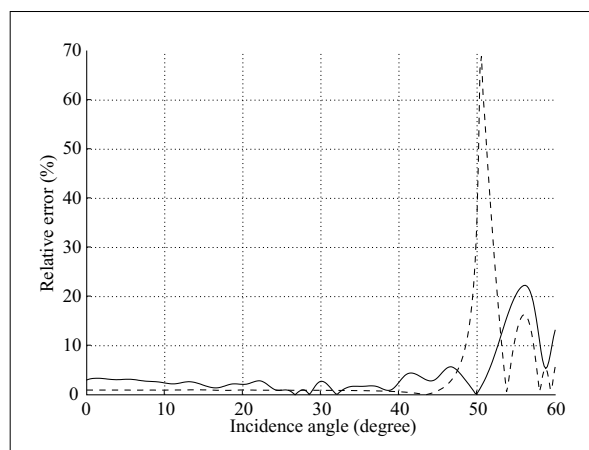


Figure 7. Discrepancies, in percentage, between the AVA curve provided by the exact solution with the AVA curve provided by our approximation (—), and between the AVA curve provided by the exact solution with the AVA curve provided by the PW reflection coefficient (- - -). (See Table I and text for the description of the medium configuration).

2.3. Results and discussion

Figure 6 depicts the amplitude-versus-angle (AVA) curves provided by the exact solution, by our approximation, and by the PW theory. A geometrical spreading compensation factor equal to $\frac{z_M}{\cos \theta}$ was applied to the predictions of our 3D approximation, and to the synthetic data provided by the 3D code OASES, in order to be compared in a suitable way with the PW predictions.

Inspection of Figure 6 shows that for small subcritical angles, AVA curves associated with the exact solution and with the PW theory are quite identical. The discrepancies

between them do not exceed 1% up to $\theta = 40^\circ$ (Figure 7). As the PW reflection coefficient varies smoothly with the incidence angle, the geometrical spreading compensation is sufficient to reduce the amplitude of the reflected wave generated by the point source to the reflected PW amplitude. The effect of the IFZ on the wave amplitude is negligible for small incidence angles in the subcritical region. Between $\theta = 40^\circ$ and the critical angle $\theta_C = 50.28^\circ$, the PW reflection coefficient rapidly increases with the incidence angle, and the geometrical spreading compensation is not sufficient anymore. The discrepancies between the exact curve and the PW reflection coefficient increase with the incidence angle and exceed 70% for θ_C (Figure 7). Therefore, the additional application of the IFZ concept becomes necessary to get the reflected P-wave amplitude.

Below and close to the critical angle, the predictions of our approximation better fit the exact solution than the PW reflection coefficient, more particularly between $\theta = 47^\circ$ and θ_C . The discrepancies between the ASA curves and the exact curves do not exceed 5% up to $\theta = 52^\circ$ and are smaller than 1% for θ_C (Figure 7). Nevertheless, with increasing incidence angle, the approximate solution shows increasing discrepancies in comparison with the exact solution. The discrepancies reach the maximum value of 22% for $\theta = 56^\circ$ (Figure 7). The explanation comes from the fact that we calculated only the reflected wave amplitude, whereas the code OASES provides the amplitude of the interference between the reflected and the head wavefields. The contribution of each wavefield to the global amplitude recorded at the receiver cannot be discriminated in the synthetic seismograms because both waves have the same traveltime for a specific range of incidence angles. For great postcritical angles, for which the signal relative to the head wave and the signal relative to the reflected wave can be separated in time, our approximation tends to the exact solutions. Our present work is focused on this topic and results will be reported later.

Note that general conclusions drawn above which are concerned with the interface model described in Table I are in fact common to other interface models with lower or stronger impedance contrasts.

Conclusion

The goal of the paper was twofold: to describe the reflector from the seismic viewpoint, or in other terms, to determine the region in the vicinity of the interface which actually affects the reflected wavefield recorded by the receivers, and to evaluate the imprint of this region on the amplitude of the reflected waves. For this purpose, the spatial region has been determined using the Fresnel volume and the Interface Fresnel zone (IFZ) concepts. It is represented by a volume of integration of properties above and beyond the interface, with a maximum lateral extent corresponding to the lateral extent of the IFZ, and with a maximum vertical extent corresponding to a thickness we have evaluated exactly and which can be greater than the seismic wavelengths. We have then calculated the amplitude of the

P-wave emanating from a point source and recorded at a receiver after its specular reflection on a smooth homogeneous interface between two elastic media. As the problem under consideration can be viewed as a problem of diffraction by the IFZ which is the physically relevant part of the interface which actually affects the reflected wavefield in this simple case, we have applied the Angular Spectrum Approach (ASA) to get the 3D analytical solution. The variation in the reflected P-wave amplitude evaluated with the ASA, as a function of the incidence angle, has been finally compared with the plane-wave (PW) reflection coefficient, and with the exact solution obtained with the 3D code OASES. For small incidence angles in the subcritical region, for which the PW reflection coefficient varies smoothly with the incidence angle, the geometrical spreading compensation has been sufficient to reduce the amplitude of the reflected wave generated by the point source to the reflected PW amplitude, and therefore the effect of the IFZ on the wave amplitude has been negligible. Nevertheless, for incidence angles close to the critical angle, for which the PW reflection coefficient rapidly increases with the incidence angle, the prediction of our approximation has better fitted the exact solution than the plane-wave reflection coefficient, which emphasizes the importance of accounting for the IFZ in amplitude calculations. Nevertheless, with increasing incidence angle, the approximate solution has shown increasing discrepancies in comparison with the exact solution because, contrary to the code OASES, we have calculated only the contribution of the reflected wavefield, without accounting for the contribution of the head wavefield.

The work presented in the paper is a preliminary step toward a “more physical” modeling of wave propagation in complex media. It identifies the volume of integration and homogeneization of the properties of the interface for which a structural description of the multi-scaled heterogeneities has to be performed for modeling the response of the interface. Our future contributions will be focused on this topic.

Acknowledgments

We would like to thank two anonymous reviewers for their relevant suggestions which have improved the paper significantly.

The work reported here is the result of discussions and fruitful collaboration with our friend Dr Eric de Bazelaire during many years. We consider ourselves extremely fortunate to have had the opportunity to work at close quarters with a scientist of his calibre, and more specially to have stroken up a profound friendship with him.

References

- [1] V. Červený: Seismic ray theory. Cambridge University Press, Cambridge, UK, 2001.
- [2] Y. Kravtsov, Y. Orlov: Geometrical optics of inhomogeneous media. Springer-Verlag, NY., 1990, (Springer Series on Wave Phenomena).

- [3] J. Schleicher, P. Hubral, M. Tygel, M. Jaya: Minimum apertures and Fresnel zones in migration and demigration. *Geophysics* **62** (1997) 183–194.
- [4] J. Spetzler, R. Snieder: The Fresnel volume and transmitted waves: a tutorial. *Geophys. J. Int.* **69** (2004) 653–663.
- [5] Y. Zhou, F. Dahlen, G. Nolet, G. Laske: Finite-frequency effects in global surface-wave tomography. *Geophys. J. Int.* **163** (2005) 1087–1111.
- [6] V. Červený, J. Soares: Fresnel volume ray-tracing. *Geophysics* **57** (1992) 902–915.
- [7] M. Kvasnička, V. Červený: Fresnel volumes and Fresnel zones in complex laterally varying structures. *J. Seism. Explor.* **3** (1994) 215–230.
- [8] M. Kvasnička, V. Červený: Analytical expressions for Fresnel volumes and interface Fresnel zones of seismic body waves. part 1: Direct and unconverted reflected waves. *Stud. Geophys. Geod.* **40** (1996) 136–155.
- [9] M. Kvasnička, V. Červený: Analytical expressions for Fresnel volumes and interface Fresnel zones of seismic body waves. part 2: Transmitted and converted waves. head waves. *Stud. Geophys. Geod.* **40** (1996) 381–397.
- [10] J. G. Hagedoorn: A process of seismic reflection interpretation. *Geophysical Prospecting* **2** (1954) 85–127.
- [11] R. Sheriff: Nomogram for Fresnel-zone calculation. *Geophysics* **45** (1980) 968–972.
- [12] J. Lindsey: The Fresnel zone and its interpretative significance. *The Leading Edge* **8** (1989) 33–39.
- [13] J. Goodman: Introduction to Fourier optics. second ed. MacGraw-Hill, 1996.
- [14] M. Born, E. Wolf: Principles of optics. 7th expanded edition. Cambridge University Press, 1999.
- [15] R. Knapp: Fresnel zones in the light of broadband data. *Geophysics* **56** (1991) 354–359.
- [16] P. Hubral, T. Krey: Internal velocities from seismic reflection time measurements. SEG, 1980.
- [17] K. Aki, P. Richards: Quantitative seismology. Second ed. University Science Books, 2002.
- [18] H. Schmidt, F. Jensen: A full wave solution for propagation in multilayered viscoelastic media with application to Gaussian beam reflection at fluid-solid interfaces. *J. Acoust. Soc. Am.* **77** (1985) 813–825.
- [19] H. Schmidt, G. Tango: Efficient global matrix approach to the computation of synthetic seismograms. *Geophys. J. R. astr. Soc.* **84** (1986) 331–359.
- [20] F. B. Jensen, W. A. Kuperman, M. B. Porter, H. Schmidt: Computational ocean acoustics. American Institute of Physics, New York, 1994.
- [21] G. Sherman: Application of the convolution theorem to Rayleigh's integral formulas. *J. Opt. Soc. Am.* **57** (1967) 546.
- [22] K. Matsushima, H. Schimmel, F. Wyrowski: Fast calculation method for optical diffraction on tilted planes by use of the angular spectrum of plane waves. *Journal of the Optical Society of America A* **20** (2003) 1755–1762.